Human Frequency-Following Response Correlates of the Distortion Product at 2F1-F2

Pritesh K. Pandya*
Ananthanarayan Krishnan[†]

Abstract

We characterized the 2F1-F2 distortion product reflected in the human frequency-following response (FFR). In the first experiment, we evaluated the input-output growth functions of the distortion product at 2F1-F2 (FFR-DP) for three primary pairs. In the second experiment, we tested the effect of primary tone level variation on the FFR-DP. The results for all three stimulus pairs showed that while the amplitude of FFR-DP increased with stimulus intensity, the slope of the amplitude growth decreased with increasing frequency. Consistent with distortion product otoacoustic emission (DPOAE) data, our observations suggest that there is a distinct region where the separation of the primary tone levels produces maximal distortion. The robust FFR-DP measure could complement the less reliable DPOAE at low frequencies and when middle ear pathology precludes its measurement.

Key Words: Auditory evoked potentials, cubic difference tone, distortion products, frequency-following response, frequency-following response distortion product, otoacoustic emissions, phase locking, temporal processing

Abbreviations: DPOAE = distortion product otoacoustic emission; FFR = frequency-following response; FFR-DP = frequency-following response distortion product

Sumario

Se realizó la caracterización del producto de distorsión 2F1-F2 reflejado en la respuesta de seguimiento frecuencial (FFR). En el primer experimento, evaluamos las funciones de crecimiento de ingreso y salida del producto de distorsión 2F1-F2 (FFR-DP) en los tres pares primarios. En el segundo experimento, evaluamos el efecto de la variación en la intensidad del tono primario en el FFR-DP. Los resultados de los tres pares de estímulos mostraron que conforme la amplitud del FFR-DP se incrementa con la intensidad del estímulo, la pendiente del incremento de la amplitud disminuye con el incremento en la frecuencia. En forma consistente con los datos de las emisiones otoacústicas por productos de distorsión (DPOAE), nuestras observaciones sugieren que existe una región particular donde la separación de los niveles del tono

---

*University of Texas at Dallas, School of Behavioral and Brain Sciences, Richardson, Texas; [†]Purdue University Department of Audiology and Speech Sciences, West Lafayette, Indiana

Reprint requests: Pritesh K. Pandya, M.A., School of Behavioral and Brain Sciences, GR 41, University of Texas at Dallas, Richardson, Texas 75083-0688; Phone: 972-883-2376; Fax: 972-883-2491; E-mail: pritesh@utdallas.edu

primario produce una distorsión máxima. Las medidas robustas del FFR-DP podrían complementar las DPOAE, menos confiables cuando se registran en frecuencias bajas o cuando la patología del oído medio impide su medición.

Palabras Clave: Potenciales evocados auditivos, tono de diferencia cúbica, productos de distorsión, respuesta de seguimiento frecuencial, producto de distorsión de una respuesta de seguimiento frecuencial, emisiones otoacústicas, cierre de fase, procesamiento temporal

Abreviaturas: DPOAE = emisión otoacústica por producto de distorsión; FFR = respuesta de seguimiento frecuencial; FFR-DP = producto de distorsión de una respuesta de seguimiento frecuencial

O ur understanding of the origin and characteristics of the 2F1-F2 distortion product is largely derived from the rather extensive animal (Kim, 1980; Kemp and Brown, 1984; Brown et al, 1987; Lonsbury-Martin et al, 1987; Martin et al, 1987) and human (Furst et al, 1988; Harris et al, 1989; Gaskill and Brown, 1990; Lonsbury-Martin and Martin, 1990; Martin et al, 1990) studies that have utilized the acoustical measure of distortion product otoacoustic emissions (DPOAE) in the ear canal. However, there are a few reported studies that have sought to evaluate the neural correlates of this cochlear nonlinearity in the responses of the auditory nerve fibers (Goldstein, 1967; Goldstein and Kiang, 1968; Kim et al, 1980; Robertson and Johnstone, 1981; Salvi et al, 1982) and in the ensemble brainstem neural activity reflected in the scalp recorded frequency-following response (Chertoff and Hecox, 1990; Rickman et al, 1991; Chertoff et al, 1992; Krishnan, 1999). The fundamental difference between the acoustic measure and the neural measure is that the former reflects nonlinearities transmitted in reverse direction from the cochlea to the ear canal and the latter reflects "forward transmitted" neural versions of presumably the same cochlear nonlinearity, albeit at two different levels along the auditory neuraxis.

In the present study, our goal was to characterize the 2F1-F2 distortion product as reflected in the human frequency-following response (FFR). The scalp recorded FFR reflects sustained neural activity phase locked to the individual cycles of the stimulus waveform among a population of neural elements in the brainstem (Worden and Marsh, 1968; Stillman et al, 1976; Moushegian et al, 1978; Hoormann et al, 1992; Galbraith, 1994; Levi et al, 1995). Although the precise neural generators remain a matter of controversy, most evidence suggests a rostral brainstem source for the human FFR (Smith et al, 1975; Sohmer et al, 1977; Stillman et al, 1978; Batra et al, 1986; Møller and Jho, 1989). The human FFR have been used to characterize subcortical asymmetries and binaural interaction components (Gerken et al, 1975; Clark et al, 1997; Krishnan and McDaniel, 1998; Ballachanda and Moushegian, 2000); evaluate neural encoding of the spectra of steady-state and time-variant speechlike sounds (Galbraith et al, 1997, 1998; Krishnan, 1999; Krishnan and Parkinson, 2000; Plyler and Ananthanarayan, 2001; Krishnan, 2002); evaluate neural encoding of pitch relevant information (Greenberg et al, 1987); and evaluate neural correlates of distortion products at F2-F1 and 2F1-F2 (Chertoff et al, 1990, 1992; Rickman et al, 1991; Krishnan, 1999).

Of particular relevance to this study are two published reports (Rickman et al, 1991; Chertoff et al, 1992) on FFR that have clearly validated the frequency-following response

distortion product (FFR-DP) at 2F1-F2 as a true neural response and not an artifact. While these authors have described the nature of the dependence of the FFR-DP amplitude on the frequency separation of the primaries (F2/F1 ratio), to our knowledge, there is only one published report of human FFR study describing the input-output behavior of the FFR-DP generated by two-tone vowel stimuli (Krishnan, 1999). In addition, the dependence of relative level of the primary signals on FFR-DP amplitude has not been reported. Thus, the present study evaluates two different aspects of the FFR-DP: (1) the input-output behavior of the FFR-DP for three different frequency pairs and (2) the effects of relative level of the primary tones on FFR-DP amplitude.

METHOD

Subjects

A total of 12 human subjects ranging in age from 19 to 25 years participated in these experiments. The criteria for inclusion in the study included: (1) hearing sensitivity of 20 dB HL or better for octave frequencies from 500 to 8000 Hz for both ears, (2) Jerger Type A tympanograms, and (3) the presence of contralateral acoustic reflexes for each ear. All subjects were unpaid volunteers.

Test Stimuli

The FFR-DP was elicited using three two-tone complex tone-burst stimuli (1. F1 = 500 Hz, F2 = 612 Hz; 2. F1 = 1000 Hz, F2 = 1225 Hz; and 3. F1 = 1400 Hz, F2 = 1715 Hz). The overall duration of each component tone burst was 80 msec, including the 10 msec rise and fall times and 60 msec plateau duration. A cosine squared gating was utilized to minimize spectral splatter of the two-tone complex. The nominal frequency values of the experimental stimuli and the constant frequency ratio of 1.225 were chosen to optimize recording of the FFR-DP and to use in future comparisons with DPOAE data. Unless otherwise indicated, the levels of the primary tones were set at L2-L1 = -5 dB. The tone bursts were digitally synthesized and controlled by a signal generation and data acquisition system (Tucker-Davis Technologies SigGen and BioSig, System II). The test stimuli were then routed through a dual channel digital-to-analog module. All
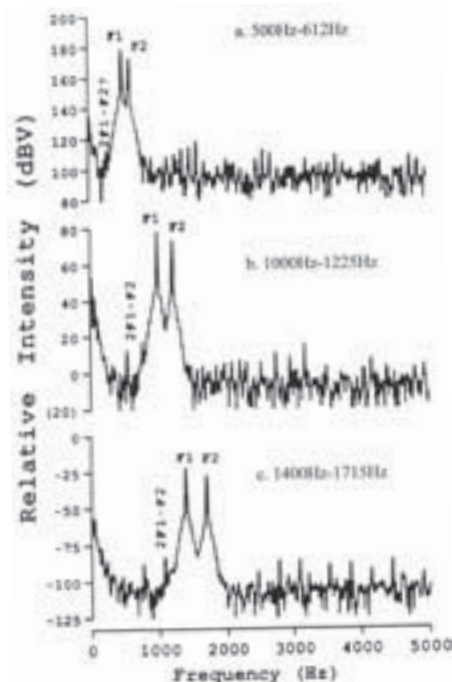
Figure 1. Acoustic spectra of the three stimulus pairs. Note that the spectral energy at 2F1-F2 is at least 60 dB below the amplitude of the F1 component.
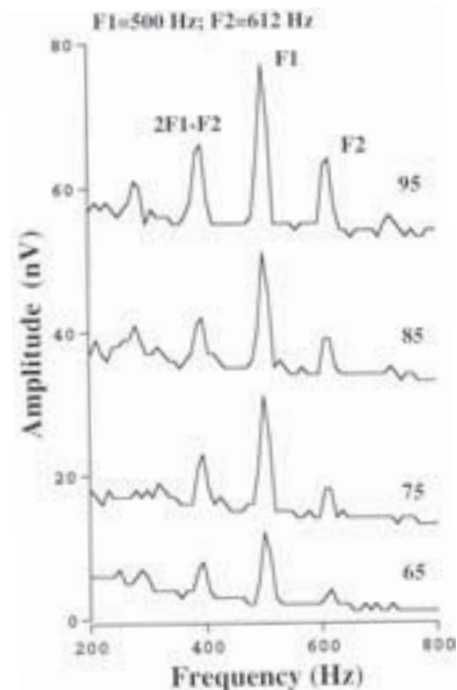
Figure 2. Mean spectrum of the derived FFRs for the 500 Hz–612 Hz primary pair plotted as function of stimulus level. Response components F1, F2, and 2F1-F2 (FFR-DP) are identified.

test stimuli were presented monaurally through magnetically shielded TDH-49 earphones encased in mu-metal to minimize electromagnetic contamination of the FFR (Ananthanarayan and Durrant, 1994).

Recording System

Subjects reclined comfortably in an acoustically shielded room after being instructed to be quiet and remain still during the recording session. The FFR-DP was recorded differentially between scalp electrodes placed on the midline of the forehead at the hairline and the 7th cervical vertebra (C7 location). An electrode on the left mastoid (A1) served as the common ground for the vertical configuration. Interelectrode impedances were maintained below 3000Ω. EEG inputs were amplified by 200,000 and bandpass filtered from 100 to 3000 Hz (6dB/octave roll-off, RC response characteristics). Each response waveform represented an average of 1500 stimulus presentations over a 90 msec analysis window using a sampling rate of 25 kHz. Sound levels are expressed as the sound pressure level measured in a 6 cc calibration cavity using a one-inch condenser microphone coupled to a sound level meter. Spectral analyses of the stimuli revealed that the acoustic energy levels at 2F1-F2 were at least 60 dB below the primary tone levels for the three two-tone stimuli (Figure 1). These levels at 2F1-F2 in the spectrum of the stimuli are well below FFR threshold.

Response Evaluation

Fast Fourier Transforms (FFTs) were performed on each of the derived frequency-following response (i.e., the waveform resulting from the subtraction of the FFR to the condensation polarity from the FFR to the rarefaction polarity in a given experimental condition) waveform obtained for the two experiments. This subtraction procedure was used to both enhance the FFR-DP and to reduce and/or eliminate the distortion component at F2-F1 (Greenberg et al, 1987; Rickman et al, 1991; Krishnan, 1999). The magnitude of the spectral peaks at F1, F2, and 2F1-F2 (reflecting magnitude of the FFR-DP) was measured for all subjects. Subsequently, mean amplitude plots for F1, F2,

and 2F1-F2 were generated to characterize the response behavior of each component.

Statistical treatment of the data involved the use of repeated-measure analysis of variance (ANOVA) with amplitude as the dependent variable. The Tukey multiple comparison test was utilized to perform post hoc analyses on the main effects that were significant. The 0.05 level of significance was selected a priori as the α level. The slope of the FFR-DP input-output functions was characterized using a linear regression algorithm.

Experimental Protocol

In the first experiment, the input-output growth functions of FFR response components were evaluated by recording the FFRs to the three different stimuli presented at 65, 75, 85, and 95 dB SPL . In the second experiment, FFRs to the 500 Hz/612 Hz stimulus pair were obtained with L1 = 85 dB SPL and for L2-L1 values of 0, -5, -10, and -15 dB. In both experiments, FFRs were obtained for both condensation and rarefaction onset polarities. The order of the primary frequencies and stimuli were counterbalanced both within and across subjects. The toneburst pairs were presented monaurally at a rate of 7.12/sec.

RESULTS

Input-Output Characteristics of F1, F2, and 2F1-F2

500 Hz–612 Hz Stimulus Pair

Three robust response components identified as F1, F2, and 2F1-F2 (FFR-DP) can be clearly seen in the spectral data shown in Figure 2. The F1 component has the largest amplitude and dominates the spectral data followed by appreciably smaller peaks at 2F1-F2 and F2. All three response components appear to increase in amplitude as intensity is increased. A more complete characterization of the amplitude behavior is shown in Figure 3. The mean amplitude of F1 and F2 (left panel) components increase in amplitude as stimulus level is increased [F1: $F(3,27 = 4.429, p < 0.0117)$, and F2: $F(3,27 = 4.673, p < 0.0094)$] with F1 showing a relatively
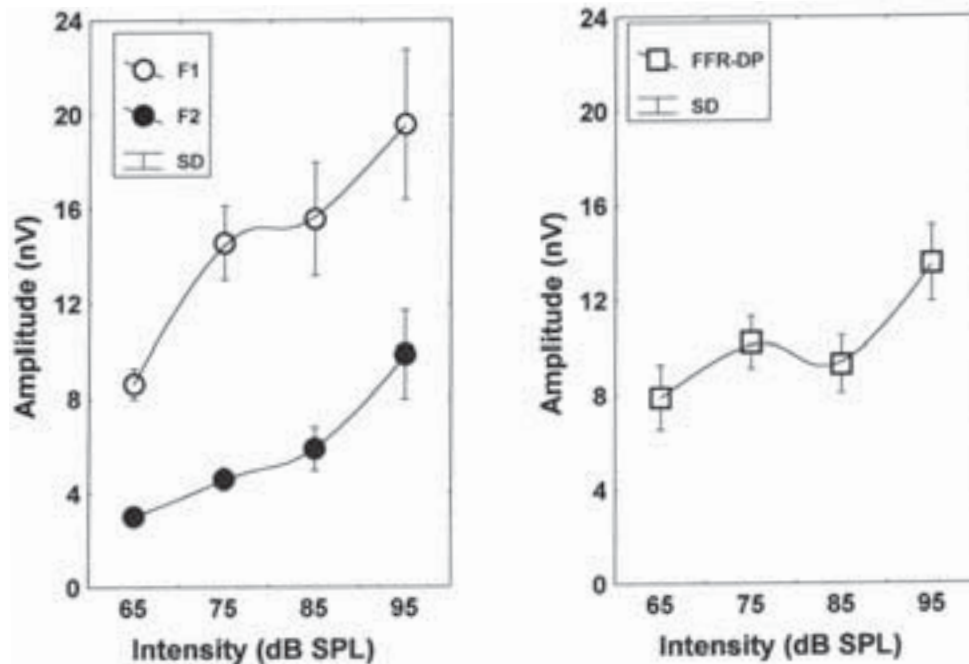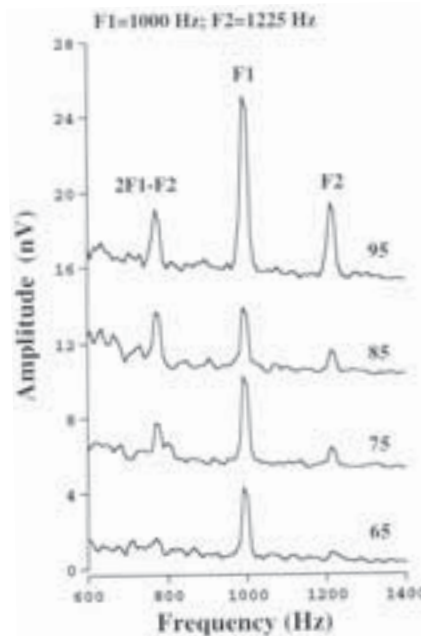
Figure 3. Mean response amplitude of F1, F2 (left panel), and FFR-DP (right panel) for the 500 Hz–612 Hz primary pair plotted as a function of stimulus level. Error bars indicate 1 S.D.

steeper amplitude growth function than F2. Tukey multiple comparison test failed to show a significant difference in the amplitude growth for F1 and F2 as the intensity was changed from 75 to 85 dB SPL suggesting a plateau in the growth function. The amplitude behavior of the FFR-DP component (right panel) is characterized by an initial gradual growth followed by an amplitude decrease at 85 dB SPL and an appreciable amplitude increment subsequently at 95 dB SPL [$F_{(3,27)}$ = 5.425, $p < 0.0078$]. Consistent with the amplitude behavior of F1 and F2, Tukey multiple comparison test showed that the FFR-DP amplitude at 75 and 85 dB SPL were not significantly different. For most stimulus levels, F1 was the largest component followed by 2F1-F2, and F2.
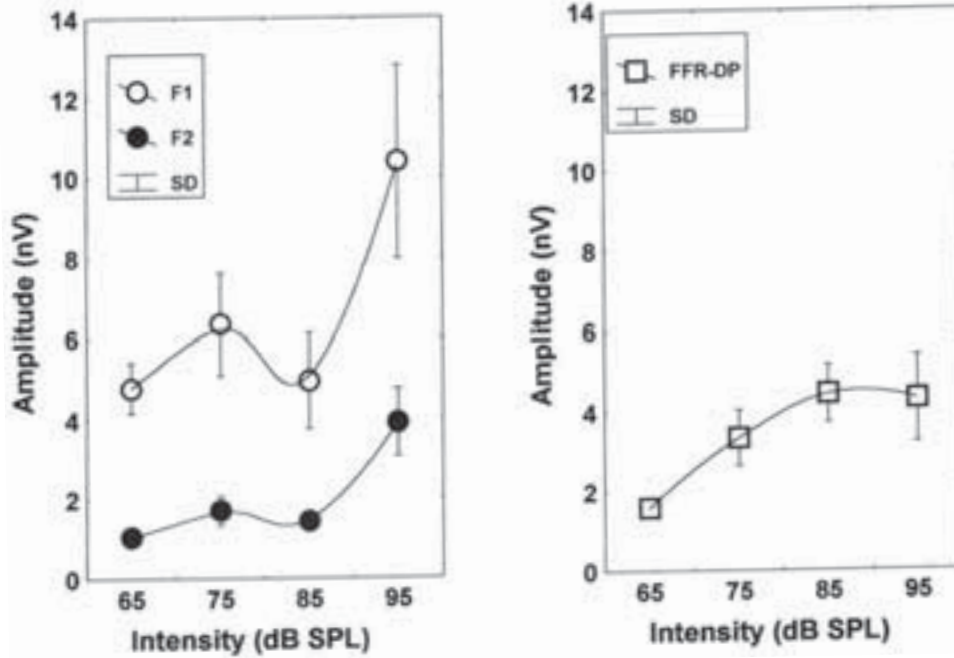
1000 Hz–1225 Hz Stimulus Pair

The mean spectral data for the 1000 Hz–1225 Hz stimuli is plotted as a function of stimulus level in Figure 4. As with the previous stimulus, clear response peaks can be identified at F1, F2, and 2F1-F2. However, unlike the data for the 500 Hz–612 Hz stimuli, the response peak corresponding to 2F1-F2 is not clearly discernible at the two lower intensities. All the three components show an apparent increase in amplitude as stim-

ulus level is increased. The mean amplitude as a function of intensity is plotted in Figure 5 for the three FFR components. The amplitude behavior of F1 and F2 (left panel) is characterized by a dip in the amplitude growth at 85 dB SPL followed by a sharp

Figure 4. Mean spectrum of the derived FFRs for the 1000 Hz–1225 Hz primary pair plotted as function of stimulus level. Response components F1, F2, and 2F1-F2 (FFR-DP) are identified.
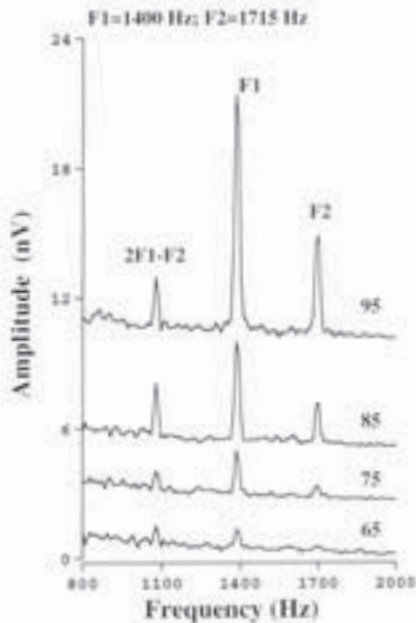
Figure 5. Mean response amplitude of F1, F2 (left panel), and FFR-DP (right panel) for the 1000 Hz–1225 Hz primary pair plotted as a function of stimulus level. Error bars indicate 1 S.D.

amplitude increase at 95 dB SPL, particularly for F1 [F1: F(3,27) = 6.348, p < 0.0021; F2: F(3,27) = 10.890, p < 0.0000]. For both F1 and F2, no significant difference in amplitude was observed at 75 and 85 dB SPL. Note that the F1 and F2 amplitudes are relatively smaller than was observed for these

Figure 6. Mean spectrum of the derived FFRs for the 1400 Hz–1715 Hz primary pair plotted as a function of stimulus level. Response components F1, F2, and 2F1-F2 (FFR-DP) are identified.
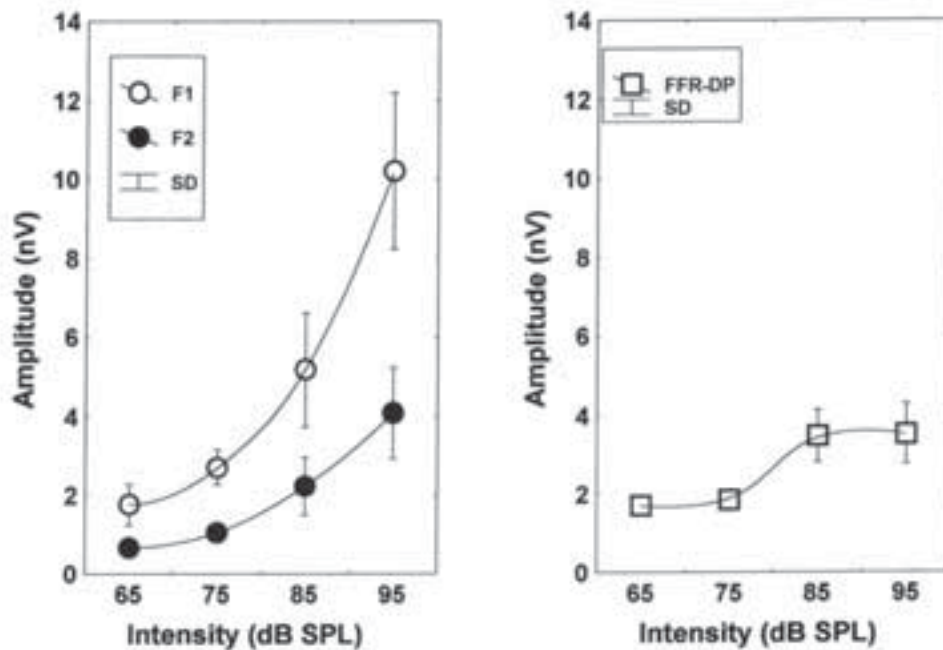
two components in response to the 500 Hz–612 Hz stimulus pair. For the FFR-DP, amplitude (right panel) increases gradually and tends to saturate at the higher intensities [F(3,27) = 5.0594, p < 0.0066)]. That this nonlinear amplitude growth is compressive in nature is suggested by the lack of a significant difference in amplitude at 85 and 95 dB SPL. Again, F1 has the largest amplitude followed by 2F1-F2 and F2.

1400 Hz–1715 Hz Stimulus Pair

Mean FFR spectra for the 1400 Hz–1715 Hz stimuli is plotted as a function of stimulus level in Figure 6. It can be seen that the amplitude of all the three components (F1, F2, and 2F1-F2) tend to increase as stimulus level is increased. The smaller amplitudes for 2F1-F2 and F2 at lower stimulus levels make these components more difficult to detect reliably. Mean amplitude of both F1 and F2 increases monotonically with stimulus level (Figure 7, left panel) with F1 showing a steeper growth than F2 [F1: F(3,27) = 9.5210, p < 0.0004; F2: F(3,27) = 5.8683, p < 0.0045]. With the exception of the amplitude change between 65 and 75 dB SPL, all other amplitude changes as a function of stimulus intensity were significant for both F1 and F2. The mean amplitude of the FFR-DP (right panel) increases gradually
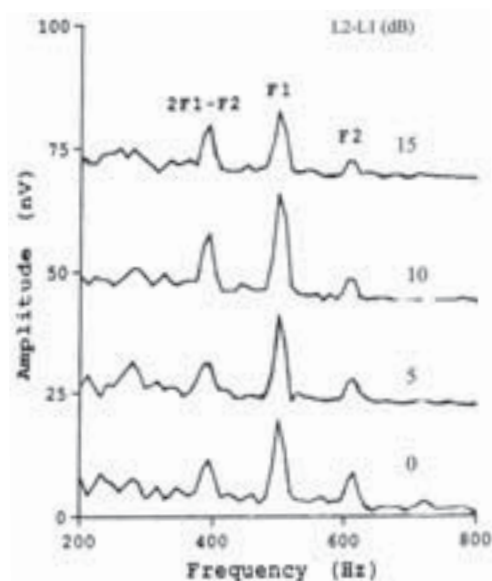
Figure 7. Mean response amplitude of F1, F2 (left panel), and FFR-DP (right panel) for the 1400 Hz–1715 Hz primary pair plotted as a function of stimulus level. Error bars indicate 1 S.D.

with intensity and tends to saturate at the higher stimulus levels [$F_{(3,27)} = 3.3875$, $p < 0.0371$]. Recall that a similar amplitude behavior was observed for the FFR-DP in response to the 1000 Hz–1225 Hz stimuli.

Effect of Relative Level on F1, F2, and 2F1-F2

The mean spectral data for the 500 Hz–612 Hz stimulus pair, plotted as a function of the level difference in the primaries (L2-L1), is shown in Figure 8. With the exception of the apparent smaller amplitude in F1 at L2-L1 = -10 dB, the magnitude of the F1 spectral peak remains essentially unaltered. As expected, the spectral peak at F2 clearly decreases as L2 level is decreased. This is not surprising, given that the level differences are due to attenuation of the L2 stimulus component relative to a constant level L1 component. The spectral peak at 2F1-F2 appears be the largest at L2-L1 = -10 dB. These observations are clearer in the mean amplitude data for F1, F2, and 2F1-F2 plotted as a function of F2 level in Figure 9. Although the mean F1 amplitude (left panel) appears to show a nonmonotonic behavior, the large variability (note the error bars) may render this characterization inaccurate. [$F_{(3,21)} = 2.4070$, $p < 0.1009$]. Consistent with the spectral data, the mean

amplitude of the F2 component decreases as L2 is decreased [$F_{(3,21)} = 3.8788$, $p < 0.0187$]. The mean amplitude of 2F1-F2 (right panel) exhibits a nonmonotonic behavior characterized by a maximum amplitude for L2-L1 = -10 dB [$F_{(3,21)} = 3.7986$, $p < 0.0330$]. Tukey multiple comparison test revealed that only the amplitude change at -10 dB relative level of F2 was significant.

Figure 8. Mean spectrum of the derived FFRs for the 500 Hz–612 Hz primary pair plotted as a function of primary tone level separation (L2-L1). Overall level of the stimulus pair was 85 dB SPL. Response components F1, F2, and 2F1-F2 (FFR-DP) are identified.
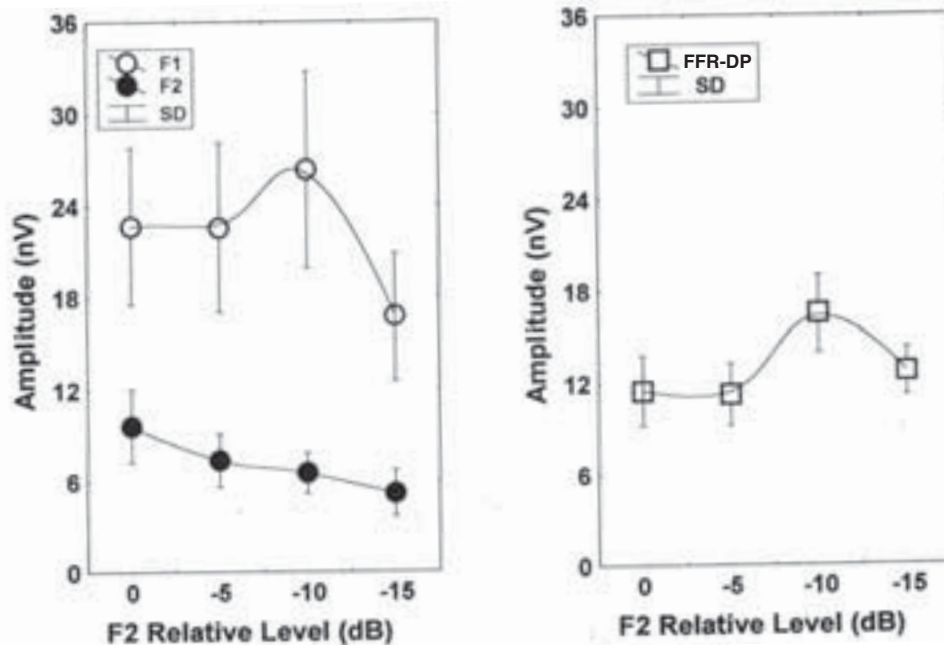
Figure 9. Mean response amplitudes of F1 and F2 (left panel), and 2F1-F2 (FFR-DP) (right panel) for the 500 Hz–612 Hz primary pair plotted as a function of primary tone level variation (L2-L1). Error bars indicate 1 S.D.

DISCUSSION

Input-Output Characteristics of F1 and F2

For all three pairs of test stimuli, the FFR spectra showed clear peaks at both F1 and F2 that increased in amplitude with intensity. The presence of robust peaks at F1 and F2 over a range of stimulus levels suggests that the sustained neural activity among a population of neural elements in the brainstem is phase locked to the individual frequency components presented in the stimulus. Phase locking as reflected in the FFR has been demonstrated for both single-frequency (Moushegian et al, 1973; Gardi et al, 1979; Ananthanarayan and Durrant, 1992) and multiple frequency stimuli (Hall, 1979; Greenberg et al, 1987; Chertoff and Hecox, 1990; Rickman et al, 1991; Chertoff et al, 1992; Krishnan, 1999; Krishnan and Parkinson, 2000; Plyler and Ananthanarayan, 2001; Krishnan, 2002). It is clear from auditory-nerve single-unit population studies that neural–phase locking is a primary basis for encoding both tonal approximations of vowels (Reale and Geisler, 1980) and synthetic speech sounds (Young and Sachs, 1979; Miller and Sachs, 1983; Sachs et al, 1983). Specifically, phase-locked activity to the formant frequencies dominates

the temporal response patterns, and a good estimate of the stimulus spectrum can be derived from these responses. Furthermore, these auditory-nerve population studies have demonstrated that distinct populations of neural elements are involved in encoding each of the formant frequencies of the speech-like sounds. Given that similar two-tone stimuli were used in this study, it is reasonable to conclude that the spectral peaks in the FFR at F1 and F2 may very well reflect phase-locked activity from distinct populations of neurons.

The growth of amplitude with intensity in our FFR data reflects an increase in the number of neural elements phase locked to the stimulus components (Krishnan and Parkinson, 2000). For the two lower frequency stimulus pairs, amplitude growth for F1 and F2 was characterized by a knee-point at 85 dB SPL. This observation is reminiscent of the characteristic input-output function for the whole nerve action potential (Yoshie and Ohashi, 1969). These investigators interpret the change in the slope of the input-output function around 75 dB SPL to suggest a change in the intensity encoding process. Specifically, the spread of excitation (once the stimulus intensity exceeds the low-frequency thresholds of the neurons innervating the inner hair cells) along the basilar membrane activates a greater number

of neurons. Consequently, the input-output function, which began to saturate somewhat at moderate intensities, grows again with further increase in intensity. The behavior of the FFR input-output function for components F1 and F2 in this study could very well reflect such a process.

We also observed that the spectral peak at F1 was the largest for all three stimuli and exhibited a steeper amplitude growth function compared to the appreciably smaller peak at F2. This dominance of the F1 response with intensity has been observed by Reale and Geisler (1980) for two-tone vowels and by Young and Sachs (1979) for synthetic vowels. These authors explain that at low intensities the temporal response is place specific and that as sound intensity is increased, the response to the formants, particularly the first formant, not only increase near their place but also spread primarily toward a place characterized by units with higher characteristic frequency. Thus, it is possible that this recruitment of higher frequency fibers to the F1 response could account for the dominance of the response at F1, not only in the single-unit population data but also in the FFR data presented here.

Finally, the amplitude of all FFR components, including the FFR-DP, decreased with increasing frequency of the stimulus pair. Several other studies have shown that FFR amplitude decreases as a function of frequency (Gardi et al, 1979; Rickman et al, 1991; Krishnan, 1999; Krishnan and Parkinson, 2000; Krishnan, 2002). Since FFR amplitude provides an index of the degree of phase locking in the neural elements that generate the FFR, this amplitude reduction may reflect a reduction in phase-locking ability with increasing frequency. In fact, no repeatable FFRs are recorded for frequencies above about 2500 Hz (Gardi et al, 1979).

Input-Output Characteristics of the FFR-DP

The FFR-DP input-output behavior for all three primaries showed essentially nonmonotonic compressive functions with the exception of the sharp amplitude increment at 95 dB for the lowest frequency (388 Hz). This is in contrast to the essentially monotonic growth function of the FFR components

generated by the primaries. Similar non-monotonic and/or diphasic input-output behavior has been reported in the rather substantial body of DPOAE research literature (Kimberley and Nelson, 1989; Harris, 1990; Lonsbury-Martin et al, 1990; Nelson and Kimberley, 1992; He and Schmiedt, 1993; Popelka et al, 1993; Stover and Norton, 1993; Kimberley et al, 1994; Popelka et al, 1995; Stover et al, 1996). These studies show that the input-output function is highly variable among subjects and within subjects for different frequency stimuli. In fact, Nelson and Kimberley (1992) identified six different input-output patterns that are prevalent in normal-hearing human ears. Even the very few auditory nerve single unit studies (Goldstein and Kiang, 1968; Kim et al, 1980) have also reported similar nonmonotonic input-output behavior of the neural 2F1-F2 distortion product.

Several possible explanations (based on cancellations due to interactions between at least two components) for some of these irregularly shaped growth functions have been offered (Norton and Rubel, 1990; Whitehead et al, 1990; Nelson and Kimberley, 1992; Popelka et al, 1993; Stover and Norton, 1993). One possibility is that a null or a notch in the DPOAE growth function at moderate levels may be the result of a destructive interaction between DPOAEs and spontaneous otoacoustic emissions (SOAEs). Alternatively, diphasic and nonmonotonic growth functions may also result from interactions between the DPOAE and other propagating distortion products at the 2F1-F2 place on the cochlear partition. Matthews and Molnar (1985) based on their modeling of intracochlear and ear canal distortion products have suggested that notches in the input-output function could result from interactions between 2F1-F2 and F2-F1 at the 2F1-F2 place. He and Schmiedt (1997) have provided evidence suggesting that the discontinuities or nonmonotonic notches in the input-output functions are related to frequency shifts in the DPOAE fine structure as stimulus level is increased. Finally, irregularly shaped input-output growth curves may be the result of two underlying cochlear mechanisms (Manley et al, 1990; Norton and Rubel, 1990; Whitehead et al, 1990). One is associated with an outer hair cell (OHC) active process for low stimulus levels

and the other, a passive nonlinear mechanism associated with the inner hair cell (IHC) subsystem for high stimulus levels. The compressive behavior, observed particularly for FFR-DP at 785 Hz and 1085 Hz in our data, is generally thought to reflect the OHC active process. Steeper input-output functions at higher stimulus intensities (observed for FFR-DP at 388 Hz) may, in part, be due to passive IHC cochlear mechanisms. It is generally accepted that at lower stimulus levels DPOAEs are dominated by active cochlear mechanical processes, and by passive cochlear mechanics at higher stimulus levels (Whitehead et al, 1990). Finally, the different amplitude behavior observed for the primaries and the FFR-DP may suggest different processes, presumably at the cochlear level, mediating these responses.

Slope of the FFR-DP Input-Output Function

Although there are inherent difficulties in direct comparison of data from neural far-field recorded responses with DPOAE data, the basis for drawing comparisons rests upon the fact that stimulus conditions are similar for both sets of data. However, these comparisons are only qualitative due to the differences in both dependent and independent variables between this data set and the relevant DPOAE data.

While human DPOAE studies have shown a wide range of input-output function slope values, the general pattern of increasing slope values with increasing frequency is clear across studies (Harris, 1990; Lonsbury-Martin et al, 1990; Nelson and Kimberley, 1992). In contrast, slopes for our FFR-DP data, in the comparable frequency regions, tended to decrease as the FFR-DP frequency increased from 388 Hz to 1085 Hz (slopes changed from 0.159 to 0.072). The steeper slope for the lowest frequency may be largely due to the sharp increase in FFR-DP amplitude at the highest intensity level. In fact, when the slope measure was repeated with the data point at the highest level excluded, the slopes across the three frequencies were comparable (slope at 388 Hz dropped to 0.069). However, the slope discrepancy between our FFR-DP data and the DPOAE data still remains. It is tempting to speculate that the discrepancy in slope

between the FFR-DP and the DPOAE could reflect fundamental differences in the response behavior of the neural and the acoustical representation of presumably the same cochlear nonlinearity in the ear canal. That these representations of cochlear nonlinearity may be different is also suggested by the observation that the FFR-DP is more robust with its peak only 20–25 dB below the primaries whereas the DPOAE peak is typically 60 dB down from the primaries in humans.

Dependence of FFR-DP on Level Separation

In addition to its dependence on the overall level of the primary stimuli, DPOAE amplitude has been shown to depend on the level difference between the primaries (Gaskill and Brown, 1990; Whitehead et al, 1995a, 1995b). The overall level of the primaries also influences this dependence on level difference. For high stimulus levels, maximum DPOAE is observed when L1 = L2 (Rasmussen et al, 1993; Whitehead et al, 1995b). For low stimulus levels, maximum DPOAE amplitude was observed when L1 was greater than L2 by about 10–15 dB (Gaskill and Brown, 1990; Whitehead et al, 1995b). Greater relative level of L1 also increases DPOAE detectability by improving the signal-to-noise ratio (Hauser and Probst, 1991). The observation of maximum FFR-DP amplitude at a level difference of 10 dB (L1-L2 = 10 dB), for our relatively high level primaries (85 dB SPL), is not entirely consistent with DPOAE data that shows maximum DPOAE amplitude when L1 = L2 for high level primaries. To the extent that this difference is real (appreciable variability in DPOAE and FFR-DP data notwithstanding), it lends additional support to the possibility that the underlying cochlear processes generating the FFR-DP and DPOAE may be different.

Clinical and Theoretical Implications

One of the limitations of DPOAE is the relative difficulty in measuring distortion products at frequencies below 1000 Hz. In contrast, FFRs in general and the FFR-DP in particular are prominent at frequencies below 1000 Hz. The FFR-DP may be used to

complement DPOAE measures in evaluating nonlinearities of the auditory system generated from more apical regions of the cochlea. An additional advantage of the neural FFR-DP measure is that it is relatively less susceptible to middle ear pathology compared to the DPOAE measure that is obscured by even a mild middle ear pathology. Of course, a disadvantage of the FFR-DP is that it would be sensitive to retro-cochlear lesions involving the auditory nerve or brainstem structures. We are currently in the process of evaluating the simultaneously recorded DPOAE and FFR-DP in an effort to determine if the underlying cochlear mechanisms are the same for these two versions of cochlear nonlinearity.

Because the FFR is most robust at physiologically relevant sound levels and its source is phase-locked discharges in nerve fibers and nerve cells, it provides a useful index of temporal processing at caudal levels of the central auditory nervous system. It is possible that the FFR and its derivatives can serve as useful complements in the assessment of disorders where impairments in temporal processing have been implicated. Although the data is currently sketchy, the FFR has been measured from individuals with dyslexia (Stillman et al, 1976; McAnally and Stein, 1996) and auditory neuropathy (Starr et al, 1991).

A more detailed understanding of how primary tones pairs (F1 and F2) interact may shed light on the generation and behavior of auditory distortion products. Technical difficulties in isolating the cochlear response to the primary tones from the stimulus energy at these frequencies preclude analyses of the behavior of F1 and F2 responses in DPOAE measures. In this study, we report the ability to evaluate the neural response behavior to the F1 and F2 primary frequency components as well as to the distortion product frequency at 2F1-F2. Unlike DPOAE measures, it is possible to evaluate distortion products at the cubic difference tone 2F1-F2 and at the difference tone F2-F1 from the same FFR due to the prominence of these components in the response spectrum. Some investigators have referred to the distortion product at the difference tone as the envelope following response (Levi et al, 1995; Dolphin et al, 1994; Dolphin, 1997). Recall that an interaction between the 2F1-F2 and F2-F1 place could affect the

fine structure of the input-output function of the FFR-DP and DPOAE. Further evaluation of this interaction may lead to a better understanding of the underlying mechanisms that influence distortion products recorded from the human auditory system.

REFERENCES

Ananthanarayan AK, Durrant JD. (1992) The frequency following response and the onset response: evaluation of frequency specificity using a forward-masking paradigm. *Ear Hear* 13:228–233.

Ananthanarayan AK, Durrant JD. (1994) Comparison of earphone radiation recorded from hearing impaired subjects and a resistor network simulator. *Br J Audiol* 28:149–154.

Ballachanda BB, Moushegian G. (2000) Frequency-following response: effects of interaural time and differences. *J Am Acad Audiol* 11:1–11.

Batra R, Kuwada S, Maher VL. (1986) The frequency-following response to continuous tones in humans. *Hear Res* 21:167–177.

Brown AM. (1987) Acoustic distortion from rodent ears: a comparison of responses from rats, guinea pigs and gerbils. *Hear Res* 31:25–37.

Chertoff ME, Hecox KE. (1990) Auditory nonlinearities measured with auditory-evoked potentials. *J Acoust Soc Am* 87:1248–1254.

Chertoff ME, Hecox KE, Goldstein R. (1992) Auditory distortion products measured with averaged auditory evoked potentials. *J Speech Hear Res* 35:157–166.

Clark JL, Moushegian G, Rupert AL. (1997) Interaural time effects on the frequency-following response. *J Am Acad Audiol* 8:308–313.

Dolphin WF. (1997) The envelope following response to multiple tone pair stimuli. *Hear Res* 110:1–14.

Dolphin WF, Chertoff ME, Burkard R. (1994) Comparison of the envelope following response in the Mongolian gerbil using two-tone and sinusoidally amplitude-modulated tones. *J Acoust Soc Am* 96:2225–2234.

Furst M, Rabinowitz W, Zurek PM. (1988) Ear canal otoacoustic distortion at 2f1-f2 from human ears: relation to other emissions and perceived combination tones. *J Acoust Soc Am* 84:215–222.

Galbraith GC. (1994) Two-channel brain-stem frequency-following responses to pure tone and missing fundamental stimuli. *Electroencephalogr Clin Neurophysiol* 92:321–330.

Galbraith GC, Bhuta SM, Choate AK, Kitahara JM, Mullen TA, Jr. (1998) Brainstem frequency following response to dichotic vowels during attention. *Neuroreport* 9:1889–1893.

Galbraith GC, Jhaveri SP, Kuo J. (1997) Speech-evoked brainstem frequency-following responses during verbal transformations due to word repetition. *Electroencephalogr Clin Neurophysiol* 102:46–53.

Gardi J, Salamy A, Mendelson T. (1979) Scalp-recorded frequency-following responses in neonates. *Audiology* 18:494–506.

Gaskill SA, Brown AM. (1990) The behavior of the acoustic distortion product, 2f1-f2, from the human ear and its relation to auditory sensitivity. *J Acoust Soc Am* 88:821–839.

Gerken GM, Moushegian G, Stillman RD, Rupert AL. (1975) Human frequency-following responses to monaural and binaural stimuli. *Electroencephalogr Clin Neurophysiol* 38:379–386.

Goldstein JL. (1967) Auditory nonlinearity. *J Acoust Soc Am* 41:676–689.

Goldstein JL, Kiang, NYS. (1968) Neural correlates of the aural combination tone 2F1-F2. *Proc IEEE* 56:981–992.

Greenberg S, Marsh JT, Brown WS, Smith JC. (1987) Neural temporal coding of low pitch. I. Human frequency-following responses to complex tones. *Hear Res* 25:91–114.

Hall JW, III. (1979) Auditory brainstem frequency following responses to waveform envelope periodicity. *Science* 205:1297–1299.

Harris FP. (1990) Distortion-product otoacoustic emissions in humans with high frequency sensorineural hearing loss. *J Speech Hear Res* 33:594–600.

Harris FP, Lonsbury-Martin BL, Stagner BB, Coats AC, Martin GK. (1989). Acoustic distortion products in humans: systematic changes in amplitudes as a function of f2/f1 ratio. *J Acoust Soc Am* 85:220–229.

Hauser R, Probst R. (1991) The influence of systematic primary-tone level variation L2-L1 on the acoustic distortion product emission 2f1-f2 in normal human ears. *J Acoust Soc Am* 89:280–286.

He N, Schmiedt RA. (1993) Fine structure of the 2f1-f2 acoustic distortion product: changes with primary level. *J Acoust Soc Am* 94:2659–2669.

He N, Schmiedt RA. (1997) Fine structure of the 2f1-f2 acoustic distortion product: effects of primary level and frequency ratios. *J Acoust Soc Am* 101:3554–3565.

Hoormann J, Falkenstein M, Hohnsbein J, Blanke L. (1992) The human frequency-following response (FFR): normal variability and relation to the click-evoked brainstem response. *Hear Res* 59:179–188.

Kemp DT, Brown AM. (1984) Ear canal acoustic and round window electrical correlates of 2f1-f2 distortion product generated in the cochlea. *Hear Res* 13:39–46.

Kim DO. (1980) Cochlear mechanics: implications of electrophysiological and acoustical observations. *Hear Res* 2:297–317.

Kim DO, Molnar CE, Matthews JW. (1980) Cochlear mechanics: nonlinear behavior in two-tone responses as reflected in cochlear-nerve-fiber responses and in ear-canal sound pressure. *J Acoust Soc Am* 67:1704–1721.

Kimberley BP, Kimberley BM, Roth L. (1994) A neural network approach to the prediction of pure tone thresholds with distortion product emissions. *Ear Nose Throat J* 73:812–823.

Kimberley BP, Nelson DA. (1989) Distortion product emissions and sensorineural hearing loss. *J Otolaryngol* 18:365–369.

Krishnan A. (1999) Human frequency-following responses to two-tone approximations of steady-state vowels. *Audiol Neurootol* 4:95–103.

Krishnan A. (2002) Human frequency following responses: representation of steady state vowels. *Hear Res* 166:192–201.

Krishnan A, McDaniel SS. (1998) Binaural interaction in the human frequency-following response: effects of interaural intensity difference. *Audiol Neurootol* 3:291–299.

Krishnan A, Parkinson J. (2000) Human frequency-following response: representation of tonal sweeps. *Audiol Neurootol* 5:312–321.

Levi EC, Folsom RC, Dobie RA. (1995) Coherence analysis of envelope-following responses (EFRs) and frequency-following responses (FFRs) in infants and adults. *Hear Res* 89:21–27.

Lonsbury-Martin BL, Harris FP, Stagner BB, Hawkins MO, Martin GK. (1990) Distortion product emissions in humans. I. Basic properties in normally hearing subjects. *Ann Otol Rhinol Laryngol Suppl* 147:3–14.

Lonsbury-Martin BL, Martin GK. (1990) The clinical utility of distortion-product otoacoustic emissions. *Ear Hear* 11:144–154.

Lonsbury-Martin BL, Martin GK, Probst R, Coats AC. (1987) Acoustic distortion products in rabbit ear canal. 1. Basic features and physiological vulnerability. *Hear Res* 28:173–189.

Manley GA, Koppl C, Johnstone BM. (1990) Components of the 2F1-F2 distortion product in the ear canal of the Bobtail lizard. In: Dallos P, Geisler CD, Matthews JW, Ruggero MA, Steele CR, eds. *The Mechanics and Biophysics of Hearing*. Berlin: Springer-Verlag, 210–218.

Martin GK, Lonsbury-Martin BL, Probst R, Scheinin SA, Coats AC. (1987) Acoustic distortion products in rabbit ear canal. II. Sites of origin revealed by suppression contours and pure tone exposures. *Hear Res* 28:191–208.

Martin GK, Probst R, Lonsbury-Martin BL. (1990) Otoacoustic emissions in human ears: normative findings. *Ear Hear* 11:106–120.

Matthews JW, Molnar CE. (1985) Modeling intra-cochlear and ear canal distortion product (2f1-f2). In: Allen JB, Hall JL, Hubbard A, Neely ST, Tubis A, eds. *Peripheral Auditory Mechanisms*. New York: Springer-Verlag, 258–265.

McAnally KI, Stein JF. (1996) Auditory temporal coding in dyslexia. *Proc R Soc Lond B Biol Sci* 263:961–965.

Miller MI, Sachs MB. (1983) Representation of stop consonants in the discharge patterns of auditory-nerve fibers. *J Acoust Soc Am* 74:502–517.

Møller AR, Jho HD. (1989) Response from the exposed intracranial human auditory nerve to low-frequency tones: basic characteristics. *Hear Res* 38:163–175.

Moushegian G, Rupert AL, Stillman RD. (1973) Scalp-recorded early responses in man to frequencies in the speech range. *Electroencephalogr Clin Neurophysiol* 35:665–667.

Moushegian G, Rupert AL, Stillman RD. (1978) Evaluation of frequency-following potentials in man: masking and clinical studies. *Electroencephalogr Clin Neurophysiol* 45:711–718.

Nelson DA, Kimberley BP. (1992) Distortion-product emissions and auditory sensitivity in human ears with normal hearing and cochlear hearing loss. *J Speech Hear Res* 35:1142–1159.

Norton SJ, Rubel EW. (1990) Active and passive ADP components in mammalian and avian ears. In: Dallos P, Geisler CD, Matthews JW, Ruggero MA, Steele CR, eds. *The Mechanics and Biophysics of Hearing*. Berlin: Springer-Verlag, 219–226.

Plyler PN, Ananthanarayan AK. (2001) Human frequency following responses: representation of second formant transitions in normal-hearing and hearing-impaired listeners. *J Am Acad Audiol* 12:423–533.

Popelka GR, Karzon RK, Arjmand EM. (1995) Growth of the 2f1-f2 distortion product otoacoustic emission for low-level stimuli in human neonates. *Ear Hear* 16:159–165.

Popelka GR, Osterhammel PA, Nielsen LH, Rasmussen A. (1993) Growth of distortion product otoacoustic emissions with primary tone level in humans. *Hear Res* 71:12–22.

Rasmussen AN, Popelka GR, Osterhammel PA, Nielsen LH. (1993) Clinical significance of relative probe-tone levels on distortion-product otoacoustic emissions. *Scand Audiol* 22:223–229.

Reale RA, Geisler CD. (1980) Auditory-nerve fiber encoding of two-tone approximations to steady-state vowels. *J Acoust Soc Am* 67:891–902.

Rickman MD, Chertoff ME, Hecox KE. (1991) Electrophysiological evidence of nonlinear distortion products to two-tone stimuli. *J Acoust Soc Am* 89:2818–2826.

Robertson D, Johnstone BM. (1981) Primary auditory neurons: nonlinear responses altered without changes in sharp tuning. *J Acoust Soc Am* 69:1096–1098.

Sachs MB, Voight HF, Young ED. (1983) Auditory-nerve representation of vowels in background noise. *J Neurophysiol* 50:27–45.

Salvi R, Perry J, Hamernik RP, Henderson D. (1982) Relationships between cochlear pathologies and auditory nerve and behavioral responses following acoustic trauma. In: Hamernik RP, Henderson D, Salvi R, eds. *New Perspectives on Noise Induced Hearing Loss*. New York: Raven, 165–188.

Smith JC, Marsh JT, Brown WS. (1975) Far-field recorded frequency-following responses: evidence for the locus of brainstem sources. *Electroencephalogr Clin Neurophysiol* 39:465–472.

Sohmer H, Pratt H, Kinarti R. (1977) Sources of frequency following responses (FFR) in man. *Electroencephalogr Clin Neurophysiol* 42:656–664.

Starr A, McPherson D, Patterson J, Don M, Luxford W, Shannon R, Sininger Y, Tonakawa L, Waring M. (1991) Absence of both auditory evoked potentials and auditory percepts dependent on timing cues. *Brain* 114:1157–1180.

Stillman RD, Crow G, Moushegian G. (1978) Components of the frequency-following potential in man. *Electroencephalogr Clin Neurophysiol* 44:438–446.

Stillman RD, Moushegian G, Rupert AL. (1976) Early tone-evoked responses in normal and hearing-impaired subjects. *Audiology* 15:10–22.

Stover LJ, Neely ST, Gorga MP. (1996) Latency and multiple sources of distortion product otoacoustic emissions. *J Acoust Soc Am* 99:1016–1024.

Stover LJ, Norton SJ. (1993) The effects of aging on otoacoustic emissions. *J Acoust Soc Am* 94:2670–2681.

Whitehead ML, Lonsbury-Martin BL, Martin GK. (1990) Actively and passively generated acoustic distortion at 2f1 - f2 in rabbits. In: Dallos P, Geisler CD, Matthews JW, Ruggero MA, Steele CR, eds. *The Mechanics and Biophysics of Hearing*. Berlin: Springer-Verlag, 243–250.

Whitehead ML, McCoy MJ, Lonsbury-Martin BL, Martin GK. (1995a) Dependence of distortion-product otoacoustic emissions on primary levels in normal and impaired ears. I. Effects of decreasing L2 below L1. *J Acoust Soc Am* 97:2346–2358.

Whitehead ML, Stagner BB, McCoy MJ, Lonsbury-Martin BL. (1995b) Dependence of distortion product otoacoustic emissions on primary levels in normal and impaired ears. II. Asymmetry in L1, L2 space. *J Acoust Soc Am* 97:2359–2377.

Worden FG, Marsh JT. (1968) Frequency-following (microphonic-like) neural responses evoked by sound. *Electroencephalogr Clin Neurophysiol* 25:42–52.

Yoshie W, Ohashi T. (1969) Clinical use of cochlear nerve action potential responses in man for differential diagnosis of hearing loss. *Acta Otolaryngol Suppl* 252:71–87.

Young ED, Sachs MB. (1979) Representation of steady-state vowels in the temporal aspects of the discharge patterns of populations of auditory-nerve fibers. *J Acoust Soc Am* 66:1381–1403.